Nuclear Magnetic Resonance Investigations of Configurational Non-rigidity in Dinuclear Platinum(IV) Complexes. Part 3.† Novel Fluxional Rearrangements in [(PtXMe$_3$)$_2$(SCHRSCHRECHR)] (X = Cl, Br, or I; R = H or Me; E = S or CH$_2$) Complexes

By **Edward W. Abel, Martin Booth, Gary King, Keith G. Orrell,* Graham M. Pring,** and **Vladimir Šik,** Department of Chemistry, University of Exeter, Exeter EX4 4QD

The title complexes have been synthesised for the first time. For the complex with R = H and E = S, X-ray and n.m.r. data indicate that the six-membered trithian ring adopts a boat conformation. Novel fluxional rearrangements in this complex have been studied by dynamic n.m.r. methods. One of these processes involves a series of 60° pivots of the cyclic ligand about individual S $\longrightarrow$ Pt bonds which averages the ligand-methylene and equatorial Pt–Me environments. The energy ($\Delta G^{\ddagger}$) of this process has been computed to be 58.6 kJ mol^{-1} and is halogen independent. A higher-energy process associated with ligand dissociation–recombination involves a scrambling of the Pt–Me groups. For the complex with R = H and E = CH$_2$, where the sulphur-pivot process cannot take place, only Pt–Me scrambling occurs. For the complex with R = Me and E = S, where the ligand ring adopts the usual chair conformation, the ligand-methyl groups prevent the pivot process from occurring at a measurable rate.

OUR recent studies [1-4] of the complexes formed by the reaction between linear bidentate organosulphur ligands MeS(CHR)$_n$SMe (R = H or Me; n = 0—2) with trimethylplatinum halides [(PtXMe$_3$)$_4$] have shown that a variety of fluxional phenomena are observable by dynamic n.m.r. spectroscopy. These molecular motions include six-membered ring reversal,[3] pyramidal ligand-atom inversion,[2-4] ligand-atom commutations,[3,4] and platinum-methyl scrambling.[3,4]

As an extension to the above work we became interested in the fluxional characteristics of the complexes formed by the reaction between [(PtXMe$_3$)$_4$] and six-membered organosulphur rings containing two or three sulphur atoms. Preliminary results have been reported [5] and we now report our detailed studies of the complexes formed with the ligands 1,3-dithian SCH$_2$SCH$_2$CH$_2$CH$_2$, 1,3,5-trithian SCH$_2$SCH$_2$SCH$_2$, and β-2,4,6-trimethyl-1,3,5-trithian β-SCHMeSCHMeSCHMe. Of particular interest is the way in which an additional unco-ordinated sulphur atom in these cyclic ligands can influence the mechanism and rate of 1,3-ligand-atom commutations between pairs of platinum(IV) atoms.

EXPERIMENTAL

Materials.—Standard literature methods [6-8] were used to prepare the ligands SCH$_2$SCH$_2$SCH$_2$, SCH$_2$SCH$_2$CH$_2$CH$_2$, and β-SCHMeSCHMeSCHMe in good yields. Reactions of the above ligands with [(PtXMe$_3$)$_4$] were carried out using standard methods [1] in all cases except with β-SCHMeSCHMeSCHMe where heptane was used as a solvent.

Spectra.—The ^{1}H n.m.r. spectra of the complexes were recorded on a JEOL PS/PFT-100 spectrometer using either CDCl$_3$ or C$_6$D$_5$NO$_2$ as solvent. A JES-VT-3 variable-temperature unit was used to control the probe temperature, which was measured to an accuracy of $\leqslant 1$ °C using a Comark digital thermometer (type 5000) attached to a Cu/Cu–Ni thermocouple adapted for use in the n.m.r. probe.

Computations.—Standard computer analyses [9] of the variable-temperature spectra were performed using modified versions [10] of the DNMR3 computer program of Kleier and Binsch.[11]

RESULTS AND DISCUSSION

Preparation and Structure of the Complexes.—The reactions of [(PtXMe$_3$)$_4$] (X = Cl, Br, or I) with SCH$_2$SCH$_2$SCH$_2$ and SCH$_2$SCH$_2$CH$_2$CH$_2$ proceeded smoothly in refluxing benzene to give the dinuclear complexes [(PtXMe$_3$)$_2$L] in good yields. Analytical data for these complexes are given in Table 1. In contrast, attempts to form similar complexes with the β-SCHMeSCHMeSCHMe using identical conditions failed. The complex [(PtClMe$_3$)$_2$(SCHMeSCHMeSCHMe)] was formed when heptane was used as a solvent, but only in 5% yield (Table 1). The analogous bromo- and iodo-complexes were shown by ^{1}H n.m.r. spectroscopy to be present in small amounts in solution, but could not be isolated in the solid state.

The low yields of the complexes [(PtXMe$_3$)$_2$-(SCHMeSCHMeSCHMe)] can be explained by recourse to the structures of the complexes [(PtXMe$_3$)$_2$L]. An X-ray crystallographic study of [(PtClMe$_3$)$_2$-(SCH$_2$SCH$_2$SCH$_2$)] [5] confirmed the dinuclear nature of the complex but additionally showed the ligand ring to have adopted a boat conformation, Figure 1. The energetic preference for the boat over the chair form is almost certainly due to the fact that the last conformer involves considerable steric interactions between the unco-ordinated sulphur atom and one of the bridging chlorine atoms. Analogous structures have been assumed for all the complexes [(PtXMe$_3$)$_2$L] (X = Cl, Br, or I; L = SCH$_2$SCH$_2$SCH$_2$ or SCH$_2$SCH$_2$CH$_2$CH$_2$) and are supported by ^{1}H n.m.r. evidence, see later.

The case of β-SCHMeSCHMeSCHMe is somewhat different. Electron and X-ray diffraction studies of the

---

† Part 2 is ref. 4.

TABLE 1

New six-membered sulphur heterocyclic complexes of halogenotrimethylplatinum(IV)

Complex	Yield/ %	Colour	M.p. (θ_c/°C) *	Analysis/% Calc. C	Analysis/% Calc. H	Analysis/% Found C	Analysis/% Found H
$[(PtClMe_3)_2(SCH_2SCH_2SCH_2)]$	72	White	235	15.7	3.50	15.7	3.45
$[(PtBrMe_3)_2(SCH_2SCH_2SCH_2)]$	60	White	220	13.9	3.10	14.0	3.05
$[(PtIMe_3)_2(SCH_2SCH_2SCH_2)]$	49	White	190	12.4	2.75	13.2	2.75
$[(PtClMe_3)_2\{SCH_2S(CH_2)_3\}]$	77	White	220	17.9	3.90	17.6	3.70
$[(PtBrMe_3)_2\{SCH_2S(CH_2)_3\}]$	61	White	217	15.8	3.45	15.6	3.40
$[(PtIMe_3)_2\{SCH_2S(CH_2)_3\}]$	35	White	220	14.0	3.05	14.0	3.10
$[(PtClMe_3)_2(SCHMeSCHMeSCHMe)]$	5	Pale yellow	172	19.7	4.15	19.9	4.10

* With decomposition.

ligand have shown it to exist in a chair conformation with the methyl groups occupying equatorial positions.[12,13] Proton n.m.r. studies confirm this structure in solution and show no evidence for the alternative chair structure with all methyl groups axial, even at very low temperatures. If the ligand retains the chair conformation in forming the complexes $[(PtXMe_3)_2L]$ two major steric interactions arise: first, involving lone pairs of the unco-ordinated sulphur atom and the bridging halogen atom X(1), and secondly between the methyl group, B, of the SCHMeS bridge and the other halogen atom, X(2) (Figure 2). Alleviation of the first interaction by adoption of the boat conformation, as in the other complexes, introduces an additional interaction between the ligand methyl groups, C and C′, and the halogen atom X(1). Alleviation of the second steric interaction by the adoption of an axial position for methyl group B, as in $[(PtXMe_3)_2(MeSCHMeSMe)]$,[3] would require the ligand ring to adopt the unfavourable chair conformation where all the methyl groups are axial, see above.

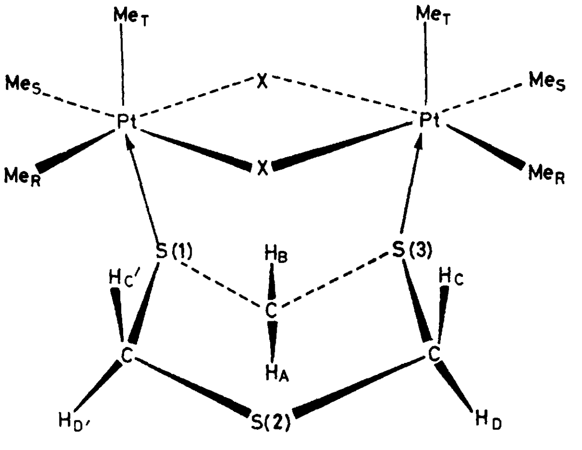

FIGURE 1 Structure of $[(PtClMe_3)_2(SCH_2SCH_2SCH_2)]$

We therefore conclude that the products formed from the reaction between $[(PtXMe_3)_4]$ and β-SCHMeSCHMeSCHMe have the structure shown in Figure 2. This sterically hindered chair structure explains the very low yield of such species which decreases further as the halogen size increases. This chair structure is supported by the magnitude of $^3J(^{195}Pt-^1H)$ couplings for the chloro-complex, see below. We should also note that a dinuclear complex is not formed between $[(PtClMe_3)_4]$ and $MeSCMe_2SMe$ [3] presumably due to analogous unfavourable steric interactions.

N.M.R. Studies.—Static spectra. All the chloro-complexes were readily soluble in $CDCl_3$ but solubility rapidly decreased in the order Cl > Br > I with the iodo-complexes being insufficiently soluble for n.m.r. purposes.

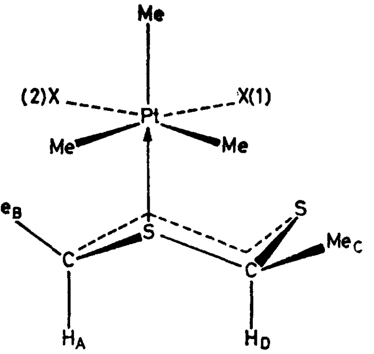

FIGURE 2 Proposed structure for $[(PtXMe_3)_2$-$(SCHMeSCHMeSCHMe)]$ viewed down Pt · · · Pt axis

Proton spectra recorded in $CDCl_3$ at −30 °C showed well resolved signals for all the complexes $[(PtXMe_3)_2L]$ (X = Cl or Br). Cooling below this temperature resulted in no further changes. Analyses of these ' static ' spectra confirm the structures described above and shown diagrammatically in Figures 1 and 2.

In the Pt–Me region three signals in the ratio 1 : 1 : 1 were observed. The case of $[(PtBrMe_3)_2$-$(SCH_2SCH_2SCH_2)]$ is shown in Figure 3. These signals arise from the three distinct Pt–Me environments, R, S,

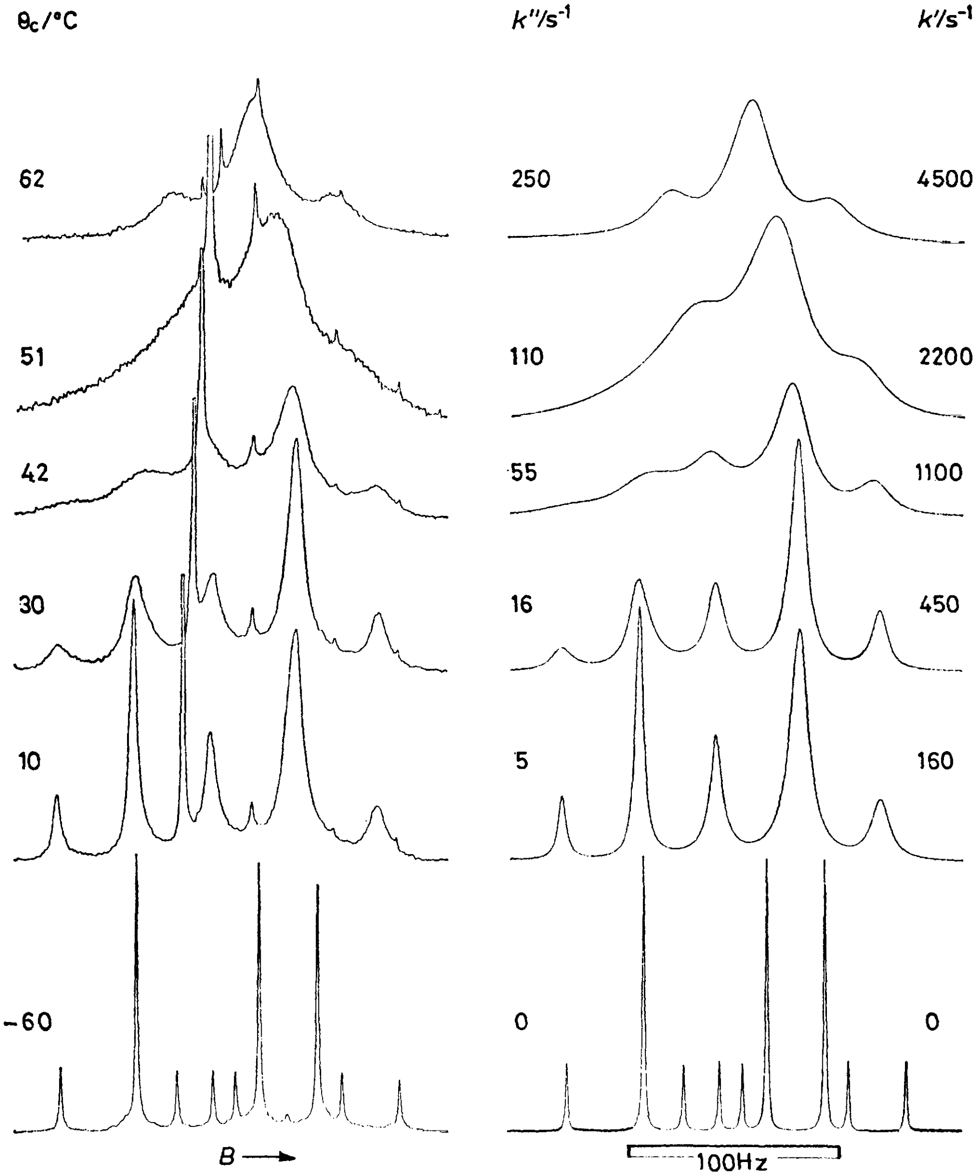

FIGURE 3 Experimental and computer-synthesised spectra of the total Pt–Me region of $[(PtBrMe_3)_2(\overline{SCH_2SCH_2SCH_2})]$

and T (Figure 1), and exhibit characteristic coupling to ^{195}Pt. The Pt–Me groups, R and S, *trans* to halogen invariably resonate at lower frequency and have the greater coupling constants $^2J(^{195}Pt–^1H)$, in agreement with values found for other dinuclear complexes.[1,14] The signal for the Pt–Me groups T, *trans* to sulphur, is at a somewhat higher frequency than the other two signals and shows a smaller $^2J(^{195}Pt–^1H)$ value in agreement with previous data.[3,14] All the ^{1}H data for the Pt–Me signals are given in Table 2. The trends in the abov ecouplings reflect *trans*- and *cis*-halogen influences as noted previously.[1,15] Finally, the Pt–Me groups, R, close to the ligand–methylene protons, C and C′, are assigned to the lowest-frequency signal in accordance with arguments used for related complexes.[4,14]

The spectra for the ligand protons are more complex than those for the Pt–Me region. Upon complexation these protons become deshielded compared to the free ligand. This deshielding is greatest in the SCHRS groups which bridge the dinuclear platinum moiety.

Consider first the spectra for the complex $[(PtClMe_3)_2(\overline{SCHMeSCHMeSCHMe})]$. The C-methyl groups give rise to two doublets in the ratio 1 : 2 corresponding to methyl groups B and C, respectively, Figure 2. The methine protons resonate at much higher frequency

TABLE 2

Proton n.m.r. parameters [a] for platinum-methyl groups in the complexes $[(PtXMe_3)_2L]$

Complex	Solvent	ν_T/Hz		ν_S/Hz		ν_R/Hz		J_{TX}/ Hz	J_{SX}/ Hz	J_{RX}/ Hz	T_2^{*} [b]/ s
		a	b	a	b	a	b				
$[(PtClMe_3)_2(SCH_2SCH_2SCH_2)]$	$CDCl_3$	163.56	+0.054	109.16	−0.014	83.11	−0.023	70.50	77.15	76.76	0.25
$[(PtBrMe_3)_2(SCH_2SCH_2SCH_2)]$	$CDCl_3$	177.24	+0.050	119.62	0.000	92.52	0.000	71.53	76.41	76.17	0.27
$[(PtClMe_3)_2(SCH_2SCH_2CH_2CH_2)]$	C_6D_5-NO_2	172.36	+0.043	115.47	+0.041	99.48	+0.062	71.29	76.29	77.37	0.29
	$CDCl_3$	162.47		108.88		93.62		71.66	76.17	77.39	
$[(PtBrMe_3)_2(SCH_2SCH_2CH_2CH_2)]$	$CDCl_3$	179.07		120.23		103.02		71.89	73.89	77.76	
$[(PtClMe_3)_2(SCHMeSCHMeSCHMe)]$	$CDCl_3$	163.57		112.15		87.12		70.80	77.21	77.51	

[a] In $CDCl_3$ or $C_6D_5NO_2$ solution relative to $SiMe_4$. Values of chemical shift (ν_i) with reference to $SiMe_4$ at temperature θ_c given by $\nu_i/\mathrm{Hz} = a + b(\theta_c/°\mathrm{C})$. [b] $T_2^{*} = (\pi\Delta\nu_{\frac{1}{2}})^{-1}$, where $\Delta\nu_{\frac{1}{2}}$ is the measured linewidth at half-height in the absence of exchange.

TABLE 3

Proton n.m.r. parameters [a] for the ligands and their complexes with $[(PtXMe_3)_4]$

Complex or free ligand	ν_A		ν_B (H or Me)		ν_C (H or Me)		ν_D		J_{AB}	J_{AX}	J_{BX}	J_{CD}	J_{CX}	J_{DX}	T_2^{*} [b]/ s
	a	b	a	b	a	b	a	b							
$[(PtClMe_3)_2(SCH_2SCH_2SCH_2)]$	522.26	−0.0410	456.20	+0.0281	487.26	+0.0505	404.46	−0.0987	−13.67	14.16	1.0	−12.30	12.40	4.0	0.19
$[(PtBrMe_3)_2(SCH_2SCH_2SCH_2)]$	550.90	−0.0437	473.75	+0.0510	498.90	+0.0510	408.40	−0.0897	−13.90	15.00	1.0	−12.0	13.0	5.0	0.18
$SCH_2SCH_2SCH_2$	408.0		408.0		408.0		408.0								
$[(PtClMe_3)_2(SCH_2SCH_2CH_2CH_2)]$	473.17		450.64						−14.16	13.5	3.0				
$SCH_2SCH_2CH_2CH_2$	382.0		382.0												
$[(PtClMe_3)_2(SCHMeSCHMeSCHMe)]$	552.20		226.75		170.59		521.24		7.63	14.0	0.0	7.02	0.0	10.3	
$SCHMeSCHMeSCHMe$	414.0		159.5		159.5		414.0		7.0			7.0			

[a] Values of chemical shift (ν_i) with reference to $SiMe_4$ in $CDCl_3$ at temperature (θ_c) given by $\nu_i/\mathrm{Hz} = a + b(\theta_c/°\mathrm{C})$; J values in Hz. [b] $T_2^{*} = (\pi\Delta\nu_{\frac{1}{2}})^{-1}$, where $\Delta\nu_{\frac{1}{2}}$ is the natural linewidth at half-height.

giving two quartet patterns which exhibit additional coupling to ^{195}Pt. It is the magnitudes of these $^3J(^{195}Pt-^1H)$ couplings which confirm the structure shown in Figure 2. The bridging proton, A, shows equivalent coupling to two ^{195}Pt atoms of magnitude 14.0 Hz. Assuming that the Karplus equation is applicable, this large coupling constant implies a H_A–C/S $\longrightarrow$ Pt dihedral angle of either *ca.* 0 or *ca.* 180°. In Figure 2 this dihedral angle is 180° for an axial group and 60° for an equatorial group. Hence the methine proton, A, is shown in the correct environment, *i.e.* axial to the ligand ring. The methine protons, D and D′, exhibit a $^3J(^{195}Pt-^1H)$ coupling of 10.3 Hz, and similar arguments show that these protons must also be in axial positions on the ring and the latter must adopt a chair conformation in order to satisfy the measured $^3J(^{195}Pt-^1H)$ values.

For the complexes $[(PtXMe_3)_2(SCH_2SCH_2CH_2CH_2)]$ the bridging methylene protons, A and B (Figure 1), give rise to an AB quartet pattern with further couplings to ^{195}Pt, the higher-frequency part of which exhibits the greater $^3J(^{195}Pt-^1H)$ value. From the Karplus equation the higher-frequency portion is assigned to the pseudo-axial proton, A, and the lower-frequency portion to the pseudo-equatorial proton, B. The spectra for the remaining six methylene protons were too complex for detailed analysis.

In contrast it is possible to fully analyse the spectra of the ligand-methylene protons for the complexes $[(PtXMe_3)_2(SCH_2SCH_2SCH_2)]$ (X = Cl or Br). The static spectrum for X = Cl is shown together with its computer simulation in Figure 4. These spectra consist of two AB quartet patterns in the ratio 1 : 2 corresponding to the two types of methylene environment. As expected the bridging methylene group, AB, absorbs at higher frequency due to the combined deshielding influences of two platinum nuclei. The pseudo-axial proton, A, absorbs at higher frequency and exhibits a large magnitude for the coupling $^3J(^{195}Pt-^1H)$ to two ^{195}Pt nuclei, implying a dihedral angle of *ca.* 180°. Similarly protons, C and C′, of the two equivalent methylene groups are also assigned to pseudo-axial environments. Spectral data for all the complexes are listed in Table 3.

Dynamic spectra. The three types of complex $[(PtXMe_3)_2L]$ (L = $SCH_2SCH_2SCH_2$, $SCH_2SCH_2CH_2CH_2$, or β-$SCHMeSCHMeSCHMe$) exhibit very different changes in their spectra above −30 °C. The complex $[(PtClMe_3)_2(SCHMeSCHMeSCHMe)]$ was first examined because it was anticipated that the methyl substituents on the ligand ring would enhance the rate of commutation of the three sulphur co-ordination sites over the dinuclear platinum moiety as in the case of the complex $[W(CO)_5(SCHMeSCHMeSCHMe)]$.[16,17] Surprisingly no change in the spectrum was observed until the temperature was above 30 °C. At these elevated temperatures

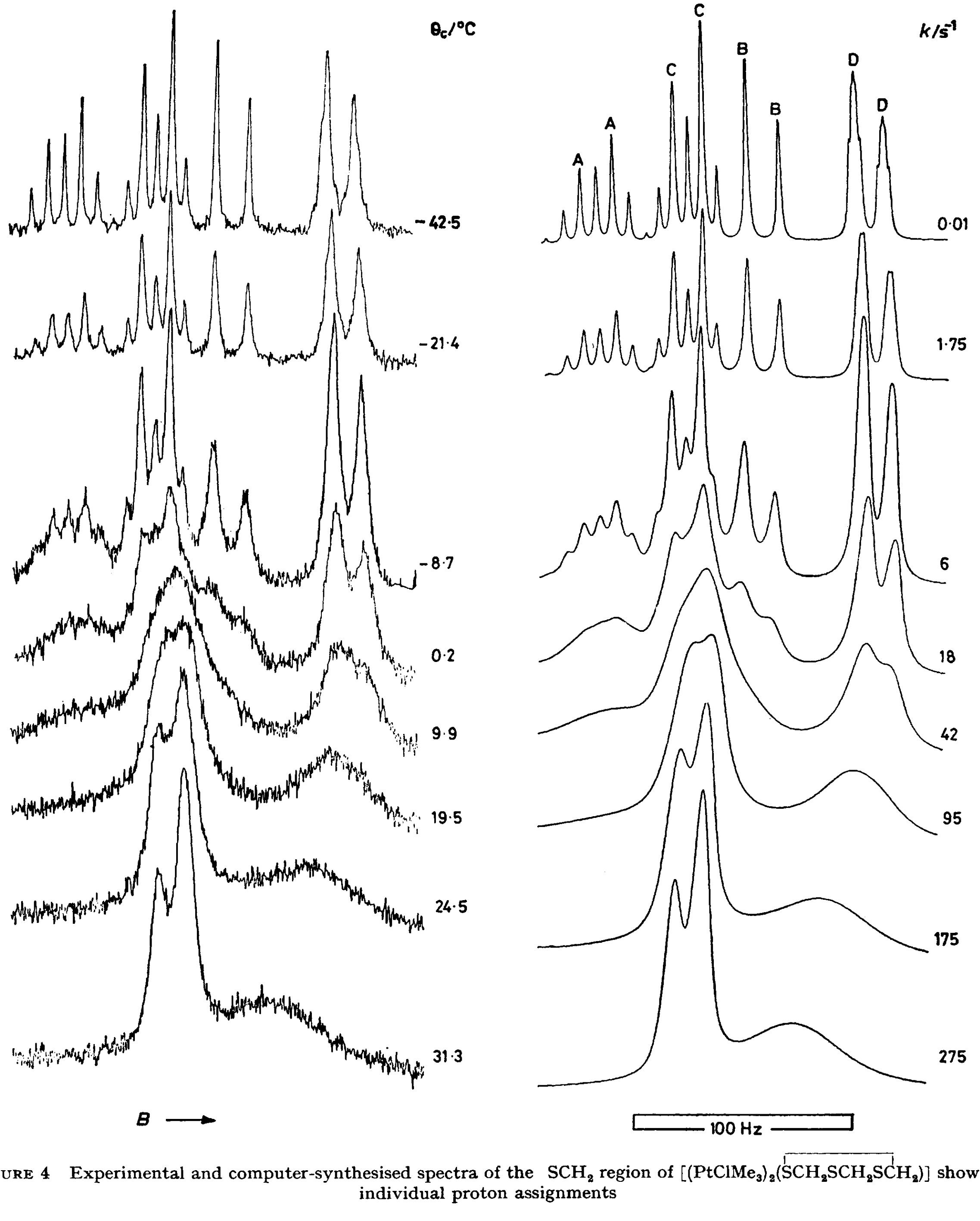

FIGURE 4 Experimental and computer-synthesised spectra of the SCH_2 region of $[(PtClMe_3)_2(\overline{SCH_2SCH_2SCH_2})]$ showing individual proton assignments

broadening of the spectral lines was observed, suggesting ligand commutation. However, a re-examination of the low-temperature spectra, after cooling from *ca.* 60 °C, showed additional peaks due to free ligand and $[(PtClMe_3)_4]$, indicating that the observed spectral changes were almost certainly a result of decomposition involving ligand dissociation.

The spectra of $[(PtXMe_3)_2(\overline{SCH_2SCH_2SCH_2})]$ were very different from those described above, with changes occurring in both ligand-methylene and platinum-methyl regions at temperatures above —30 °C (Figures 3—5). We will consider first the Pt–Me region, Figures 3 and 5. Upon raising the temperature the two equatorial Pt–Me signals coalesce to give a single broad line at about 10 °C (Figure 5). At least three possible mechanisms can be envisaged to account for such an averaging process. These include: (1) a process which permutes the pairs of sulphur co-ordination sites of the ligand ring over the dinuclear platinum moiety, (2) a synchronous or correlated double inversion of both co-ordinated sulphur

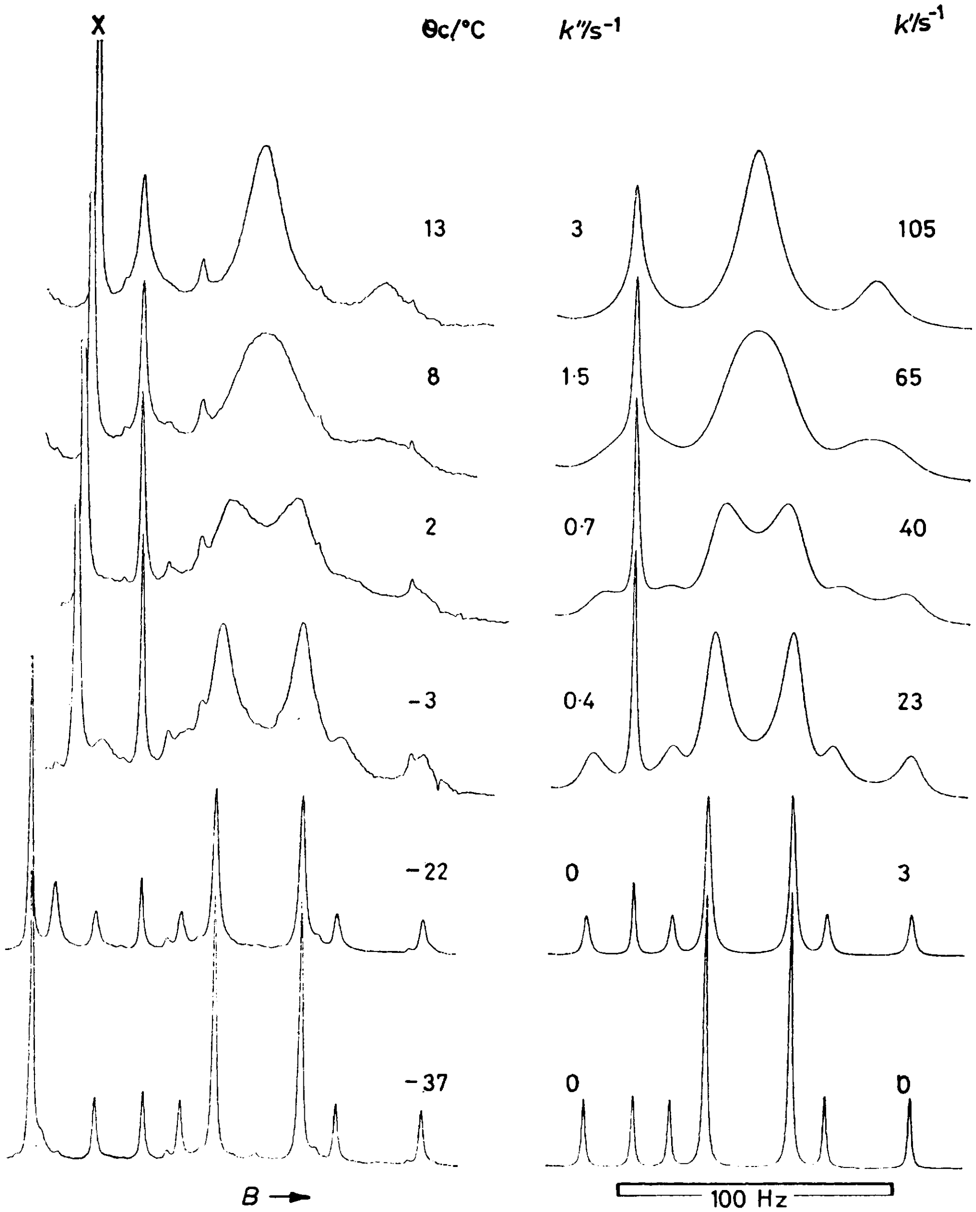

FIGURE 5 Experimental and computer-synthesised spectra of the equatorial Pt–Me region of $[(PtBrMe_3)_2(SCH_2SCH_2SCH_2)]$

atoms, and (3) dissociation–recombination of the ligand. Process (2) can be discounted because the changes in the methylene region are incompatible; (3) can also be ruled out since ^{195}Pt coupling to the ligand-methylene protons is retained. This leaves process (1) involving a series of 1,3-shifts of the cyclic ligand so that all three sulphur atoms share the co-ordination to the platinum atoms at higher temperatures.

Above 15 °C for the complex with X = Br and above 25 °C for X = Cl, a second fluxional process is observed which averages the axial Pt–Me signal with the averaged equatorial Pt–Me signal. The limiting high-temperature spectrum consists of a single Pt–Me signal with accompanying satellites, Figure 3. This second coalescence phenomenon must be due to scrambling of the three Pt–Me groups [3,4] for which the dynamic spin problem is as shown below, where k' is the rate of the 1,3-shift process and k'' the rate of Pt–Me scrambling. Synthesising the spectra in this way gave good fits of the Pt–Me region between –30 and 70 °C (Figures 3 and 5) and enabled energy-barrier data to be calculated in the usual way (Table 4).

Changes in the ligand-methylene region occur at the same time as the averaging of the Pt–Me environments. These changes involve the averaging of proton A with D and D', and of proton B with C and C'. This type of exchange confirms the boat conformation of the ligand ring since if the ring were in the chair conformation the assignments of protons C and D, and C′ and D′, would be reversed, due to a change in dihedral angle, giving a different set of dynamic spectra.

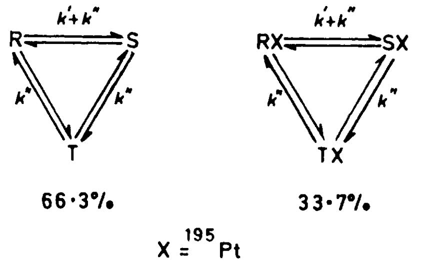

The cause of this exchange between methylene-proton environments as well as the averaging of the equatorial Pt–Me environments is thought to be a fluxion involving the commutation of all three sulphur co-ordination sites over the dinuclear platinum moiety. This motion can proceed *via* one of two possible mechanisms, namely a series of 120° twists of the ligand ring relative to the dinuclear platinum moiety, or a series of pivots through angles of 60° about any one $S \longrightarrow Pt$ bond which interchange co-ordinated and unco-ordinated sulphur-atom pairs. These two molecular motions are shown diagrammatically in Figure 6 together with the dynamic nuclear-spin problem. It is clearly seen that averaging of the methylene environments is brought about by either mechanism. However, the twist mechanism *does not* average the two equatorial Pt–Me environments and we therefore conclude that the fluxional mechanism actually operating is a pivot process about single $S \longrightarrow Pt$ bonds.

TABLE 4

Arrhenius and activation parameters for the complexes [(PtXMe$_3$)$_2$L]

Complex	Process	E_a / kJ mol^{-1}	log$_{10}A$	$\Delta H^‡$ / kJ mol^{-1}	$\Delta S^‡$ / J K^{-1} mol^{-1}	$\Delta G^‡$ * / kJ mol^{-1}
[(PtClMe$_3$)$_2$(SCH$_2$SCH$_2$SCH$_2$)]	Pivot	62.55 ± 1.17	13.49 ± 0.22	60.25 ± 1.16	5.65 ± 4.15	58.57 ± 0.08
	Methyl scrambling	84.39 ± 1.34	15.12 ± 0.22	81.76 ± 1.35	35.69 ± 4.25	71.12 ± 0.08
[(PtBrMe$_3$)$_2$(SCH$_2$SCH$_2$SCH$_2$)]	Pivot	61.79 ± 1.49	13.32 ± 0.29	59.54 ± 1.48	2.48 ± 5.47	58.80 ± 0.16
	Methyl scrambling	75.94 ± 0.72	14.29 ± 0.13	73.45 ± 0.74	20.24 ± 2.49	67.42 ± 0.01
[(PtClMe$_3$)$_2$(SCH$_2$SCH$_2$CH$_2$CH$_2$)]	Methyl scrambling	94.15 ± 3.12	15.54 ± 0.47	91.28 ± 3.11	42.96 ± 9.02	78.47 ± 0.43

* Calculated for $T = 298.15$ K.

The dynamic nuclear-spin problem for the methylene protons may be simplified as shown below. It should be noted however (Figure 6) that whereas only one pivot is required to average the Pt–Me environments two pivots are required to average the methylene environments. Therefore the rate of Pt–Me averaging will be twice the rate of methylene averaging at any given temperature. Moreover, if k' denotes the rate constant for a single pivot the ' best-fit ' rate constant for the ligand-methylene region will be half that for the Pt–Me region.

The experimental spectra could be accurately fitted in this way up to temperatures of 35 °C in the case of the chloro-complex (Figure 4) and up to 20 °C in the case of the bromo-complex. Above these temperatures the additional process of dissociation–recombination of the ligand ring referred to earlier becomes evident causing averaging of the pseudo-axial and -equatorial protons on the same carbon atom, *i.e.* $A \rightleftharpoons B$ and $C,C' \rightleftharpoons D,D'$. This dissociation–recombination process will also enhance the rate at which the Pt–Me groups R and S are averaged. However, these groups are already efficiently averaged by the pivot mechanism and hence the Pt–Me spectra were found to be insensitive to the rate of R,S exchange ($k' + k''$).

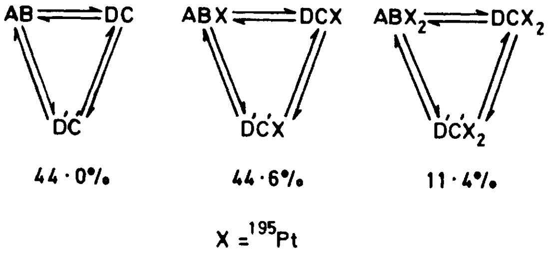

Examples of fits for both the Pt–Me and methylene regions are shown in Figures 3—5. The data obtained in this way were subjected to a least-squares analysis to give the Arrhenius and activation parameters listed in Table 4. The errors in $\Delta G^‡$ were calculated from the standard deviation term $|\sigma(\Delta H^‡) - T\sigma(\Delta S^‡)|$ as described by Binsch and Kessler.[9]

In the case of [(PtClMe$_3$)$_2$(SCH$_2$SCH$_2$CH$_2$CH$_2$)], spectra were recorded between 20 and 140 °C in C$_6$D$_5$NO$_2$. The spectra exhibited no change in either Pt–Me or ligand-methylene regions up to 50 °C. Above this temperature both regions broadened and coalesced. At 140 °C a single sharp peak with ^{195}Pt satellites was observed in the methyl region, whilst the methylene region resembled the free-ligand spectrum, no coupling to ^{195}Pt being observed. We therefore conclude that above 50 °C the ligand ring

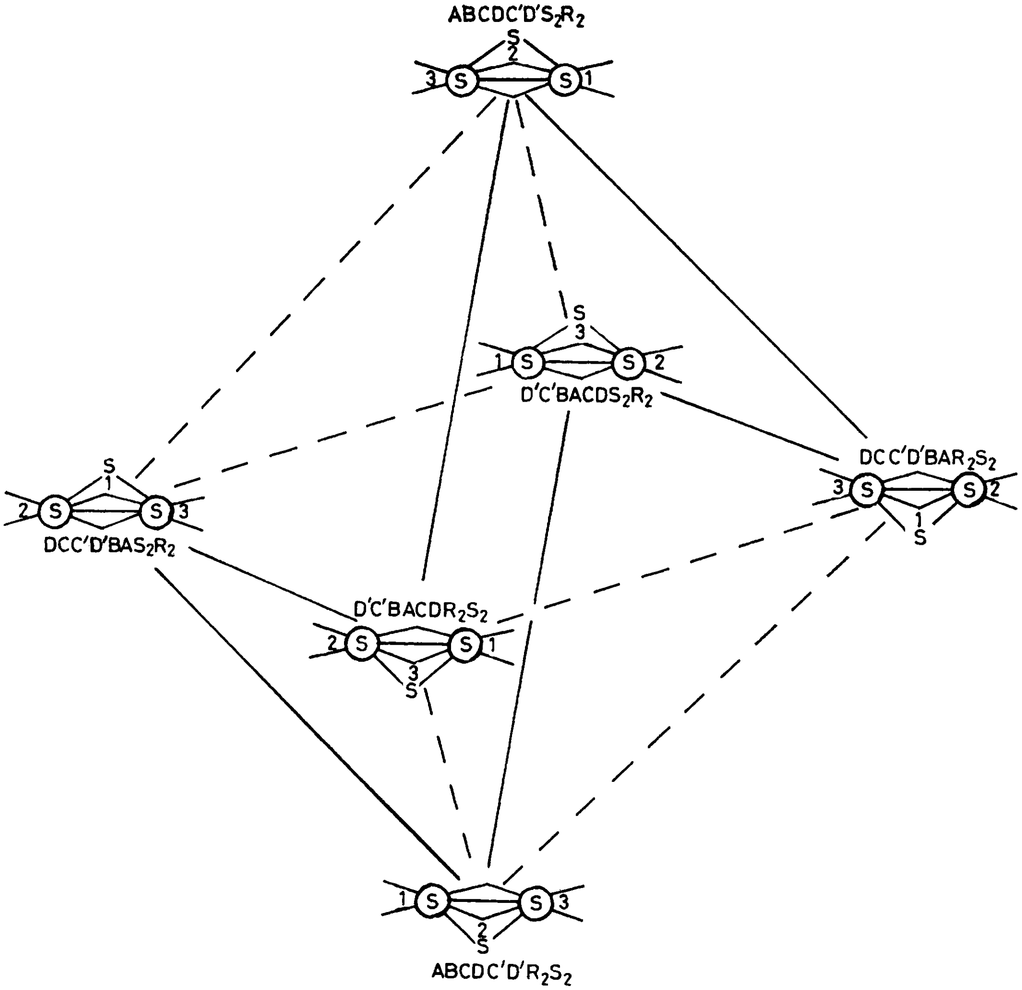

FIGURE 6 Possible fluxional mechanisms of $[(PtXMe_3)_2(\overline{SCH_2SCH_2SCH_2})]$; the labelling of the protons is as in Figure 1. (——), Pivot; (— — —), twist

dissociates from the dinuclear platinum moiety producing a five-co-ordinate platinum(IV) species which exhibits a scrambling of the methyl environments. The energy for this process is given in Table 4.

Energies and Mechanisms of the Fluxional Processes.—We have shown that for the complexes $[(PtXMe_3)_2(\overline{SCH_2SCH_2SCH_2})]$ the process which causes averaging of the three sulphur-atom co-ordination sites is a 60° pivot about individual S ⟶ Pt bonds rather than a 120° twist/rotation of the whole ligand ring. This is not unexpected since the last process involves a greater angular movement and the breaking and reforming of two S ⟶ Pt bonds as opposed to a single bond in the case of the pivot process. Furthermore, rotation about S ⟶ Pt bonds is fairly unrestricted as it is invariably fast on the n.m.r. time scale for complexes of Pt^{II} and Pt^{IV} with open-chain ligands.[10] Further consideration of the pivot process suggests that the most likely mechanism involves an intermediate with the ligand ring adopting a chair conformation, since the unco-ordinated sulphur lone pair is then in a more favourable position to form a new S ⟶ Pt bond. A possible mechanistic scheme is outlined in Figure 7. The energy of this chair conformation must be appreciably greater than that of the boat form in order to account for its lack of detection by n.m.r. spectroscopy at −30 °C. In this figure the chair conformer is shown with an energy of *ca.* 10 kJ mol^{-1} above that of the boat form. This corresponds to a chair population of *ca.* 1% at −30 °C which represents the approximate minimal detectable level of this species. It is likely, however, that the energy of this chair form is considerably greater than this. Since the chair form is not detected it is impossible to determine the height of the energy barrier ($\Delta G^{\ddagger}$) between the two forms. However, a maximum value of *ca.* 46 kJ mol^{-1} can be postulated for this parameter from data for ring reversal in the free ligand.[18]

In the light of the above discussion it is perhaps surprising that the complex $[(PtClMe_3)_2(\overline{SCHMeSCHMeSCHMe})]$ exhibits an immeasurably slow rate of ligand pivot since the ligand ring is already in the chair conformation. This implies a large increase in the energy of transition-state species compared to the chair conformation, Figure 7, due to steric requirements of the ligand-methyl groups. The height of this energy barrier must exceed *ca.* 70 kJ mol^{-1} otherwise a pivot process would be detectable before irreversible decomposition of the complex commences above 30 °C.

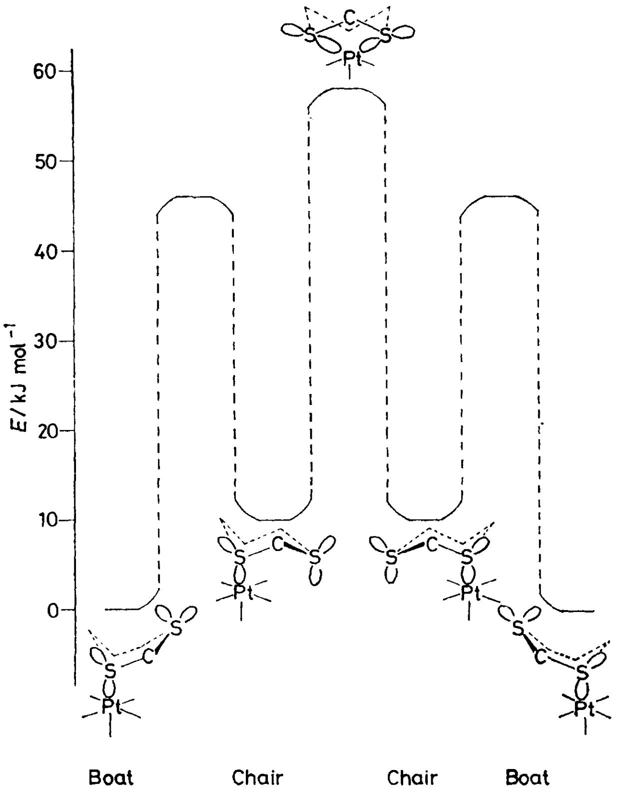

FIGURE 7 Potential-energy profile for the pivot process in $[(PtXMe_3)_2(SCH_2SCH_2SCH_2)]$

It is of considerable interest to compare the energy (58.6 kJ mol^{-1}) for the pivot process in $[(PtClMe_3)_2(SCH_2SCH_2SCH_2)]$ with the energies obtained for the analogous ligand-switching process in the dinuclear complexes with linear chalcogen ligands:[3,4] $[(PtClMe_3)_2(MeSCHMeSMe)]$ (71.5), $[(PtClMe_3)_2(MeSeCHMeSeMe)]$ (72.7), $[(PtClMe_3)_2(MeSSMe)]$ (61.3), and $[(PtClMe_3)_2(MeSeSeMe)]$ (65.2 kJ mol^{-1}). It is clear that in cases where a carbon atom separates the two sulphur atoms the energy for the pivot process is much lower than that for the switching process. There are two possible explanations for this: (*i*) for the switching process two S ⟶ Pt bonds are broken and reformed compared to a single S ⟶ Pt bond for the pivot process; and (*ii*) in the pivot process the ligand is required to rotate through 60° compared to the 180° rotation required for switching to occur.

Furthermore the switching energy is less when no carbon atom exists between the two co-ordinated chalcogen atoms, which may well reflect the different distances through which the chalcogen lone pairs are required to move in going from one ground state to the other in the two complexes. It is possible to use similar arguments concerning magnitudes of lone-pair movements to explain the increase in switching energy when sulphur atoms are replaced by selenium atoms, although in both instances other factors may well make significant contributions to the energy changes.

The energy of the pivot process is independent of the bridging halogen atoms, Table 4. In contrast, ligand-switching energies for the dinuclear complexes $[(PtXMe_3)_2(MeSCH_2SeMe)]$ are halogen dependent:[19] X = Cl (70), Br (69), or I (66 kJ mol^{-1}). This difference reflects the fact that in a switching process the chalcogen atoms move right across the plane containing the bridging halides, whereas in the pivot process this does not occur and precise location of the bridging halide atoms is unimportant.

The values of $\Delta G^\ddagger$ for the Pt–Me scrambling process listed in Table 4 are similar to those obtained previously for other dinuclear platinum complexes.[3,4] In these earlier studies the scrambling process was considered to arise from random cleavage of the Pt–X bridge bonds leading to highly fluxional five-co-ordinate platinum(IV) species.[20] However, it was also suggested that the ligand-switching and methyl-scrambling phenomena might be correlated processes in view of the close similarity of their energy parameters. More recent data[19] lend further support to this idea, in which case it is not necessary to postulate halogen-bridge breaking since the weakly bound seven-co-ordinate platinum(IV) intermediate of the ligand-switching process can itself induce Pt–Me scrambling.

In the present compounds both the switching and S-inversion processes are prevented by steric factors and hence Pt–Me scrambling can only occur by halogen-bridge breaking or by ligand dissociation–recombination, both processes producing the highly fluxional five-co-ordinate platinum(IV) species. Since we no longer favour halogen-bridge breaking, the methyl scrambling in these cyclic ligand complexes is thought to arise as a result of a breaking the S ⟶ Pt bonds. The rate of this scrambling is fastest for the 1,3,5-trithian complexes where the rapid pivot motion leads to a more weakly co-ordinated ligand which can dissociate more readily than $[(PtClMe_3)_2(SCH_2SCH_2CH_2CH_2)]$ where the pivot does not occur.

Support for the suggestion of the scrambling process being associated with ligand dissociation may be obtained from the $\Delta S^\ddagger$ values (Table 4) which are sizeably positive. These are in striking contrast to the majority of the $\Delta S^\ddagger$ values reported for pyramidal inversion and ligand switching[3,4] which are not significantly different from zero, as expected for such purely intramolecular rate processes.[21] Large positive $\Delta S^\ddagger$ values imply that the transition-state species for the process concerned possesses more vibrational and rotational degrees of freedom than the ground-state species and this is very likely to be the case for a dissociation–recombination mechanism.[22]

We therefore feel confident in concluding that the averaging of all three Pt–Me environments in these dinuclear platinum(IV) complexes occurs only when the S ⟶ Pt bonds are drastically weakened, either as a result of intra- and inter-metallic inversion (as occurs in the linear chalcogen-ligand complexes [3,4,19]) or by dissociation of the S ⟶ Pt bonds (as in these cyclic chalcogen-ligand complexes).

[1/387 *Received*, *9th March*, 1981]

REFERENCES

[1] E. W. Abel, A. R. Khan, K. Kite, K. G. Orrell, and V. Šik, *J. Chem. Soc., Dalton Trans.*, 1980, 1169.

[2] E. W. Abel, A. R. Khan, K. Kite, K. G. Orrell, and V. Šik, *J. Chem. Soc., Dalton Trans.*, 1980, 1175.

[3] E. W. Abel, A. R. Khan, K. Kite, K. G. Orrell, and V. Šik, *J. Chem. Soc., Dalton Trans.*, 1980, 2208.

[4] E. W. Abel, A. R. Khan, K. Kite, K. G. Orrell, and V. Šik, *J. Chem. Soc., Dalton Trans.*, 1980, 2220.

[5] E. W. Abel, M. Booth, S. Cameron, K. G. Orrell, and G. M. Pring, *J. Chem. Soc., Chem. Commun.*, 1981, 29.

[6] R. W. Bost and E. W. Constable, *Org. Synth.*, 1943, **Coll. vol. 2**, 610.

[7] E. Campaigne, N. F. Chamberlain, and B. E. Edwards, *J. Org. Chem.*, 1962, **27**, 135.

[8] E. J. Corey and D. Seebach, *Org. Synth.*, 1970, **50**, 72.

[9] G. Binsch and H. Kessler, *Angew. Chem. Int. Edn. Engl.*, 1980, **19**, 411.

[10] E. W. Abel, A. K. Ahmed, G. W. Farrow, K. G. Orrell, and V. Šik, *J. Chem. Soc., Dalton Trans.*, 1977, 47.

[11] D. A. Kleier and G. Binsch, *J. Magn. Reson.*, 1970, **3**, 146; D. A. Kleier and G. Binsch, DNMR3, Program 165, Quantum Chemistry Program Exchange, Indiana University, 1970.

[12] O. Hassel and H. Viervoll, *Acta Chem. Scand.*, 1947, **1**, 149.

[13] G. Halle, V. Busetti, M. Mammi, and G. Carazzolo, *Acta Crystallogr., Sect. B*, 1969, **25**, 1631.

[14] A. R. Khan, Ph.D. Thesis, University of Exeter, 1979.

[15] D. E. Clegg, J. R. Hall, and G. A. Swile, *J. Organomet. Chem.*, 1972, **38**, 403.

[16] W. A. Schenk and M. Schmidt, *Z. Anorg. Allg. Chem.*, 1975, **416**, 311.

[17] E. W. Abel, M. Booth, K. G. Orrell, and G. M. Pring, *J. Chem. Soc., Dalton Trans.*, 1981, 1944.

[18] J. E. Anderson, *J. Chem. Soc. B*, 1971, 2030.

[19] E. W. Abel, K. Kite, K. G. Orrell, V. Šik, and B. L. Williams, *J. Chem. Soc., Dalton Trans.*, in the press.

[20] D. E. Clegg, J. R. Hall, and N. S. Ham, *Aust. J. Chem.*, 1970, **23**, 1981; N. S. Ham, J. R. Hall, and G. A. Swile, *ibid.*, 1975, **28**, 759.

[21] A. Rauk, L. C. Allen, and K. Mislow, *Angew. Chem. Int. Ed. Engl.*, 1970, **9**, 400.

[22] A. A. Frost and R. G. Pearson, ' Kinetics and Mechanism,' 2nd edn., Wiley, New York, 1961.